Measurement of the ^{210}Po production induced by thermal neutron capture on ^{209}Bi

A. Letourneau [1] , G. Fioni, F. Marie, D. Ridikas

CEA Saclay, DSM/DAPNIA/SPhN, 91191 Gif-sur-Yvette, France

P. Mutti

Institut Laue-Langevin, 38000 Grenoble, France

Abstract

A measurement of the polonium production in a solid Bi target, placed in a high thermal neutron flux of 2.3 10^{13} n/cm^2/s, was performed. Two different activation methods, based on α and γ spectroscopy, were used to cross check the results. Values of (16.08 $\pm$ 1.8) mb and (18.4 $\pm$ 0.9) mb for the ^{210}Po (i.e. $^{210gs}Bi$) formation cross section were obtained and a recommended value of (17.9 $\pm$ 0.8) mb was proposed. Our results are in disagreement with adopted cross section values in the main nuclear data libraries, namely smaller by 25% for $^{210gs}Bi$. These new values will account for more precise evaluations of ^{210}Po formation in moderated spallation targets containing ^{209}Bi.

Key words: Radiative capture, Neutron sources, Spectroscopy
PACS: 25.40.Lw, 29.25.Dz

1 Introduction

In the prospect of the development of accelerator-driven systems (ADS) for nuclear waste transmutation, energy production or intense neutron sources, reliable data are essential for a correct estimate of the radiotoxicity produced in the conversion target. In particular, the use of eutectic Pb-Bi (LB) for spallation neutron-production target is directly related to the production of α-radioactive emitters of which ^{210}Po and ^{210m}Bi are the most important. In

[1] Corresponding author. Tel.:+33 1 69 08 76 01; fax: +33 1 69 08 75 84; E-mail address: aletourneau@cea.fr

such a target, due to an effective conversion of the incident proton energy into many neutrons (Letourneau et al., 2000) with energies distributed with a non negligible thermal component, ^{210}Po and ^{210m}Bi are mainly produced via the radiative neutron capture on ^{209}Bi:

$$^{209}Bi(n,\gamma)^{210gs}Bi \underset{5.013\ d}{\overset{\beta^-}{\longrightarrow}} {}^{210}Po$$

$$^{209}Bi(n,\gamma)^{210m}Bi$$

Recently, an estimate of the effect of 800 MeV energy protons on a 1 MW power LB target (Gai et al., 2000) shows that at the end of the operation time (6 months) a total specific coolant activity of 500 Ci/kg could be reached. This activity reduces after 5 years to 2.7 Ci/kg and reaches the radiotoxicity of natural uranium (69 mCi/kg) only in 300 years. Among the wide spectrum of radionuclides produced by the multiple reactions involved in the intra- and inter-nuclear cascade of the incident proton, the most dangerous are gaseous and volatile radiotoxic nuclei which can evaporate from the target in case of accident and confinement rupture. ^{210}Po with a half-life of $T_{1/2} = 138.4$ days, is one of the most dangerous because of its ability to evaporate from the LB target in the form of PbPo molecule for instance, whereas ^{210m}Bi with a half-life of $T_{1/2} = 3.04\ 10^6$ years, is non-volatile but will contribute to the long-term radiotoxicity. It should be stressed that the contribution of ^{210}Po to the total activity depends drastically on how the neutron energies are distributed in the target because the radiative cross section decreases with increasing energy. Thus in the presence of a D_2O moderator surrounding the target, i.e. with about 40% of thermal neutrons, the radiative neutron capture process is enhanced as compared to the case without moderator. For this reason, the ^{210}Po activity at the end of the operation time and after 6 months of cooling contributes to about 2% and 40%, respectively, of the total activity in presence of a moderator, whereas it contributes to only 2% after 6 months of cooling, in absence of moderator.

In this context, the precise determination of $^{209}Bi(n,\gamma)^{210gs}Bi$ and $^{209}Bi(n,\gamma)^{210m}Bi$ thermal neutron capture cross sections is essential to estimate the radiotoxicity in an ADS, in particular when moderated neutrons are used as in the case of the MEGAPIE project (Salvatores et al., 1999). In the data-bases, only three measurements of the $^{209}Bi(n,\gamma)^{210gs}Bi$ cross section have been reported with discrepancies larger than the error bars of the measurements. A value of (15 ± 3) mb was found by Seren et al. (1947), (20.5 ± 1.5) mb was found by Colmer et al. (1950) and finally Takiue et al. (1978) have reported a value of (24.2 ± 0.4) mb. All these measurements were based on a direct counting of the β^- particles issued from the decay of $^{210gs}Bi$. In contrary no direct experimental measurement exists concerning the $^{209}Bi(n,\gamma)^{210m}Bi$ cross section. This observation has lead us to start an experimental program of which ^{210}Po

thermal formation cross section is a part.

In this paper we report the results of two independent integral measurements to obtain the ^{210}Po production value in a high thermal neutron flux and the $^{209}Bi(n,\gamma)^{210gs}Bi$ cross section. These measurements are based on an α and γ-spectroscopy of ^{210}Po. The α-spectroscopy technique has already been used by Igashira et al. (2001) to measure the values of the latter cross section at 30 keV and 450 keV. However, it is the first time that such a technique is used to measure the thermal neutron capture on this element.

2 Description of the method

The principle of an activation method to measure neutron capture cross sections is to determine the number of atoms of interest produced in the sample during the irradiation and to determine the neutron flux characteristics (energy distribution and absolute intensity). For integral measurements, as we have performed in both experiments, the knowledge of the latter quantity is essential in order to determine the differential cross sections from the average values measured. But as we will see in the forward development, within our experimental conditions, this precise knowledge was not very essential and could be bypassed. The experiments have consisted in measuring the number of ^{210}Po atoms produced after irradiation of ^{209}Bi samples. The thermal neutron flux was monitored by the standard $^{59}Co(n,\gamma)^{60}Co$ reaction.

As shown on Fig. 1, ^{210}Po is formed via the β-decay of the ground state of ^{210}Bi, created by the neutron capture on ^{209}Bi. This channel is responsible for 100% of the $^{210gs}Bi$ decays, whereas the α-decay channel contributes to less than $(1.34 \pm 0.1)\ 10^{-4}$% of the decays (Harmatz, 1981). We can then assume that all $^{210gs}Bi$ nuclei formed during the irradiation are transmuted into ^{210}Po nuclei. The decay of ^{210}Po nucleus takes place through the emission of 5304.38 keV and 4516.58 keV α-particles (Browne, 1992) with respective intensities of 99.9988% and $(1.22 \pm 0.04)\ 10^{-3}$ %, forming ^{206}Pb in its ground state and first excited state. The latter level deexcitates integrally to the fundamental state via the emission of a 803.1 keV γ-ray so that this transition has an absolute intensity of $(1.21 \pm 0.04)\ 10^{-3}$ % per ^{210}Po decay.

The number of ^{210}Po atoms contained in the sample after the irradiation is proportional to the activity measured through the α or γ-ray rates. In experimental conditions, where the burn-up of the sample as well as secondary captures on $^{210gs}Bi$ and ^{210}Po can be neglected, the ^{210}Po activity Po(t), as a

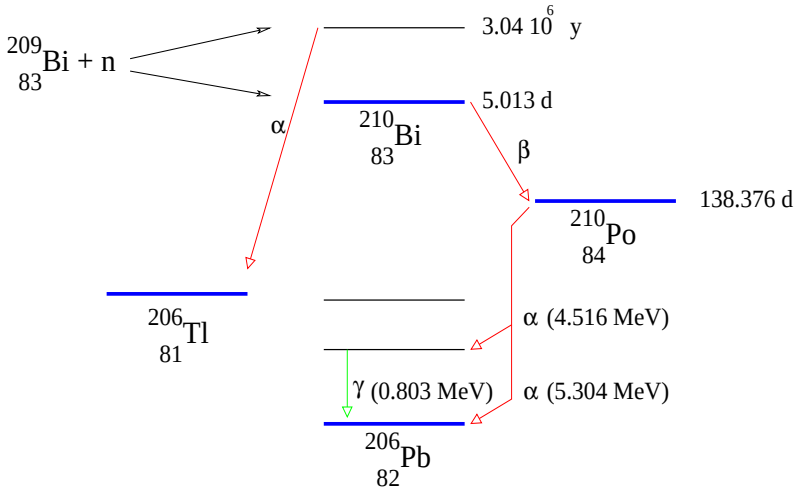

Fig. 1. Formation and decay scheme of ^{210}Po nuclei after a neutron capture on ^{209}Bi.

function of irradiation time T and cooling time t, is given by :

$$Po(t) = \frac{N_{209}\ \overline{\sigma}_{gs}\phi}{\lambda_B - \lambda_P}\{\lambda_B(1-e^{-\lambda_P T})e^{-\lambda_P t} - \lambda_P(1-e^{-\lambda_B T})e^{-\lambda_B t}\}\ , \quad (1)$$

where λ_P and λ_B are the decay constants of ^{210}Po and $^{210gs}Bi$, N_{209} the number of ^{209}Bi atoms in the target and $\overline{\sigma}_{gs}$ the average cross section for the formation of $^{210gs}Bi$ (i.e. ^{210}Po). In this equation we have neglected the α-decay of $^{210gs}Bi$ which is negligible compared to the β-decay.

The neutron flux introduced in Eq. 1 is measured separately with a standard ^{59}Co flux monitor. Because the half-life of the ^{60}Co isotope ($T_{1/2}$ = 1925.1 days) is long enough compared to a typical irradiation and cooling time, its decay could be neglected. By applying the same assumptions as before, the activity equation of ^{60}Co is reduced to :

$$Co(t) = N_{59}\ \overline{\sigma}_{Co}\phi(1-e^{-\lambda_{Co}T})e^{-\lambda_{Co}t}\ , \quad (2)$$

where N_{59} refers to the initial concentration of ^{59}Co atoms in the target and $\overline{\sigma}_{Co}$ to the average capture cross section .

If the sample and the monitor are irradiated in the same flux conditions, then from Eq. 1 and 2 we can extract the $^{210gs}Bi$ formation cross section:

$$\overline{\sigma}_{gs} = \overline{\sigma}_{Co}\,\frac{N_{59}}{N_{209}}\,\frac{Po(t)}{Co(t)}\,\frac{(\lambda_B-\lambda_P)(1-e^{-\lambda_{Co}T})e^{-\lambda_{Co}t}}{\{\lambda_B(1-e^{-\lambda_P T})e^{-\lambda_P t}-\lambda_P(1-e^{-\lambda_B T})e^{-\lambda_B t}\}} \quad (3)$$

It should be noticed that the proportionality between $\overline{\sigma}_{gs}$ and $\overline{\sigma}_{Co}$, in Eq. 3, is a direct consequence of the assumption that the burn-up for both elements could be considered as negligible. Another important point that should be stressed is that the average cross section values $\overline{\sigma}_{gs}$ and $\overline{\sigma}_{Co}$ could be replaced by differential values if resonances are sufficiently far from the region of interest, which makes the measurements independent of the neutron gas temperature. For ^{209}Bi and ^{59}Co elements, resonances are distributed above 800 eV and 150 eV, respectively, so that the g-factors are very similar for both elements (1.0004 and 1.0005). Therefore, from our integral measurements, the extraction of cross sections corresponding to discrete neutron energies (E_n=0.025 eV for instance) was allowed.

The sources of errors associated with the activation method appear clearly in Eq. 3. The main terms are the error on the cross section of the monitor ($\overline{\sigma}_{Co}$) and the errors associated to the determination of the activities. Then come the errors on the number of atoms in the samples and finally, the errors on the half-lives, the irradiation and cooling times. In principle, the latter errors are negligible in comparison with the previous ones.

3 Description of the experiments and data taking

We have performed two independent irradiations in the T4 irradiation position located at the top level of the high flux reactor at ILL (Laue-Langevin Institute, Grenoble) during two distinct cycles. The T4 position is outside the heavy water reactor vessel at about 1.3 meters from the fuel element and gives access to a perfectly thermalized neutron flux of 2.3 10^{13} n/cm^2/s.

As shown in Fig. 2, which are the results of calculations with Monte-Carlo code (MCNP Briesmeister, 1993), the thermal neutron flux accessible in the T4 position follows a pure maxwellian distribution corresponding to a temperature of 20 ^{o}C. Moreover, it is very similar to the thermal component of the neutron flux inside a 1 MW LB target operating with 800 MeV incident protons and surrounded by moderator.

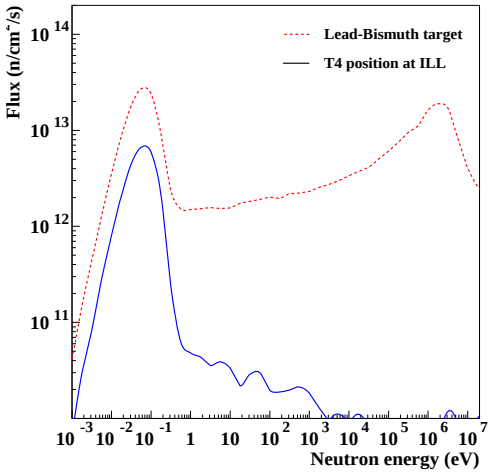

Fig. 2. Comparison of a typical neutron flux distribution produced by 800 MeV protons impinging on a 1 MW spallation Pb-Bi target, surrounded by moderator (dashed line), with the neutron flux distribution available in the T4 position at ILL (solid line). Both distributions are the results of calculations with MCNP (Briesmeister, 1993).

3.1 α-spectroscopy measurement

The determination of the ^{210}Po concentration via its α-decay is the most direct way to get access to this quantity. It requires the use of a very thin target of ^{209}Bi in order to avoid absorption and important degradation of the peak resolution due to the very short range (15 μm) of the α-particles in the ^{209}Bi foil.

Thus we have used a very thin ^{209}Bi-target of 1.1 μm in thickness obtained by the evaporation of 1 mg of pure ^{209}Bi (99.99%), with an uniformity of 2%, on a thick (0.125 mm) Ni backing. A Ni ring with 0.125 mm thick and 8 mm in diameter was stacked on the deposit in order to collimate the α-emission from the target and thus to define an exact emission surface and volume. With this geometry, an equivalent mass of (0.539 ± 0.01) mg of ^{209}Bi was in direct sight of the detector. The sample was placed in an Al container (22 mm in diameter and 62 mm in height) together with a (7.71 ± 0.01) mg foil of Al-0.1% Co alloy to monitor the neutron flux. The container was filled with He gas to limit a possible evaporation of Po by oxidation from the target. The ensemble was irradiated for 3 days and the measurements were performed 84 days after the end of the irradiation. Thanks to the high neutron flux, 3 days of irradiation were sufficient to get a good statistic.

The α-particles coming from the Po decay were collected at different distances from the target with a 300 μm thick Passivated Silicon Detector. The energy resolution of the detector given by the constructor was 15 keV at 5486 keV.

All the measurements were done in the Mini-INCA vacuum chamber (10^{-5} bar) installed at ILL (Marie et al., 2005).

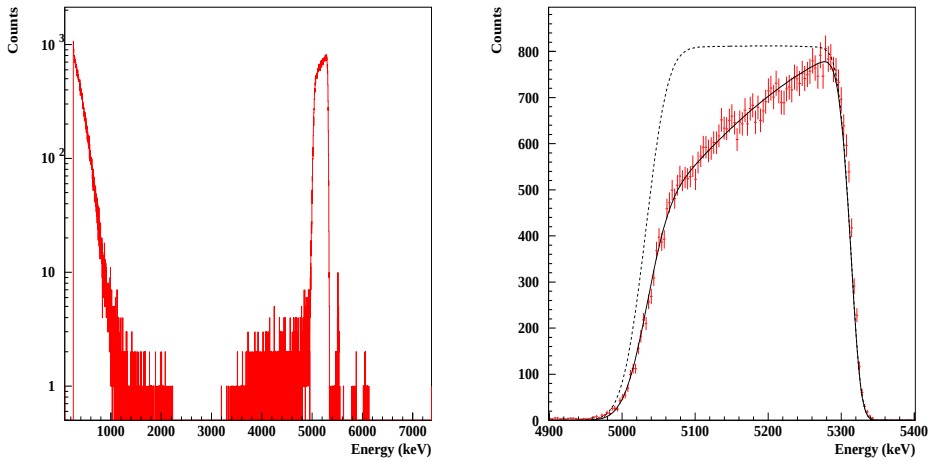

Fig. 3. a) Left: Energy spectra collected with the silicon detector positioned at a distance of 5 cm from the Bi target. b) Right: zoom-in on the 5304-keV α-ray. The experimental data are fitted with a function resulting from the convolution of a gaussian function with a parabolic decreasing step function (solid line). The dashed line is the same function but by replacing the parabolic curve with a constant step function (see text).

The α-energy spectra collected by the detector at a distance of 5 cm is shown on Fig. 3a. The peak corresponding to the most probable α particle (5304.38 keV) is clearly well separated from the low energy background originated from the interaction of β-decay particles with the detector. In Fig. 3b a zoom-in on the α-energy spectra shows the shape of the spectra with a resolution of 250 keV which is much higher than the resolution of the detector (15 keV) and a decreasing slope. The enlargement of the resolution is a consequence of the degradation of the energy when the α-particle goes through the target (energy-straggling) and depends on its thickness: the larger the distance travelled by the particle, the wider its energy distribution. Thus, when converted in distance, the resolution reflects the thickness of the target. In absence of degradation of the trajectory, the probability to detect particles in a given solid-angle should be equal whatever the depth of the emission. Thus the energy spectra should be enlarged but flat. The decreasing slope could then be attributed to a loss of detected particles due to a trajectory-straggling in the target. The energy-straggling has the effect to damage the gaussian resolution of the detector and could be modelled by an asymmetric gaussian function with a variance depending on the energy (Eq. 4). The detected energy spectra in absence of trajectory-straggling should then be modelled by a function resulting from the convolution of this asymmetric gaussian function ($G(E' - E, \sigma(E'))$) and a step function. In order to introduce the trajectory-straggling we have

replaced the step function by a parabolic-decreasing step function:

$$f(E) = \int_{E_{min}}^{E_{max}} G(E' - E, \sigma(E')) \cdot (1 - \alpha E' - \beta E'^2) dE' \ , \qquad (4)$$

where

$$\sigma(E') = \begin{array}{c} \sqrt{2\sigma_0^2 + (\gamma \cdot (E_{max} - E'))^2} \ for E' < E \\ \sqrt{\sigma_0^2 + (\gamma \cdot (E_{max} - E'))^2} \ for E' \geq E \end{array} ,$$

with σ_0 the intrinsic resolution of the detector. E_{max}, E_{min}, α, β and γ were the free parameters of the fit.

An evaluation of the particle loss has been done for all the distances by fitting the function $f(E)$ on the data (solid line in Fig. 3b) and by switching off the parabolic decrease (dashed line). By this procedure, the counting rate does not depend on the depth of the α-emission. The difference between the solid and dashed surfaces gives the yield of α-particles lost, which amounts to $(19.67 \pm 0.5)\%$ of the total recorded α yield at 5 cm.

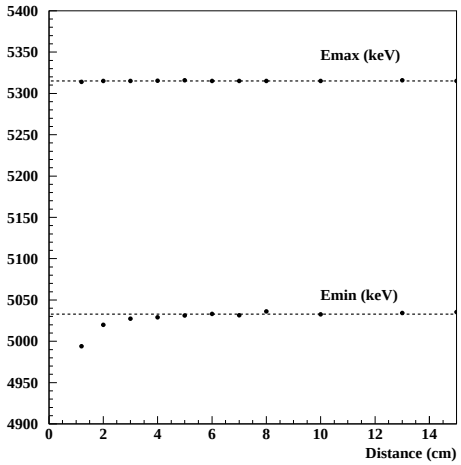

Fig. 4. Width of the α-energy spectra obtained at different distances from the fit of the experimental data with the function described by the Eq. 4. The errors are contained within the symbol size. The dashed lines indicate the mean boundaries E_{min} and E_{max}.

As shown on Fig. 4 which is one result of the fit as a function of the distance, the width of the α-energy spectra is unchanged beyond 5 cm. Below this limit, the α-collimator is less efficient and additional contributions appear in the spectrum (enlargement of the spectrum at low energy). This can be understood as a contribution of α-particles coming from the collimated region

and which become "visible" because of the trajectory-straggling. The same conclusions could be applied concerning the slope of the spectra which becomes independent of the distance beyond 5 cm so that the value given previously is representative of the correction factor applied at each distances.

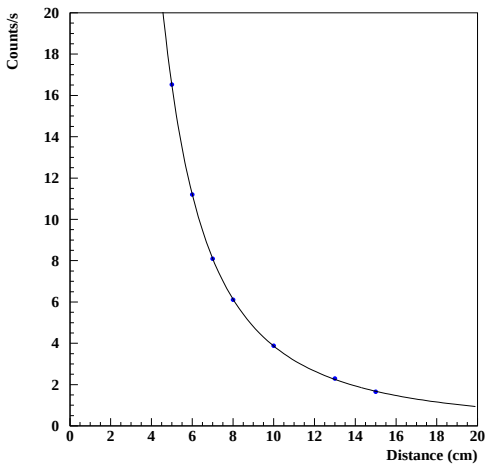

Fig. 5. Measured (symbols) and calculated (line) α-ray counts in the detector as a function of the distance from the target. Experimental error bars are contained within the size of the symbols. The calculated line is a fit to the data, with only the activity as a free parameter.

Due to the large value of the correction factor and the causes of the lost not fully established a correction factor of 10 ± 10 % was applied on measured activities. The Po activity was then deduced from the adjustment of the α-counting rate measured at different position (d $\geq$ 5 cm) and corrected for the particle loss, with a point-like emission solid angle function (solid line on Fig. 5) given by :

$$\frac{d\Omega}{4\pi} = \frac{A}{2}(1 - \frac{1}{\sqrt{1 + \frac{\nu^2}{4d^2}}}) \, , \tag{5}$$

where $\nu = 1.13$ cm is the diameter of the detector. A, the activity of the sample, is the only free parameter of the fit. This procedure, described in (Deruelle et al., 2002), allows to reduce statistical errors associated with each measurement at a given position. Thanks to a Monte-Carlo simulation where particles were equally emitted from the surface of the target defined by the collimator, it has been shown that beyond 5 cm the solid angle deduced from a point-like emission is comparable within less than 0.01% error to the emission from the surface of the target. The result, with the above adjustments, gives an activity of (5179 ± 518) Bq.

A less direct method to determine the ^{210}Po concentration in the target is by counting the γ-ray coming from the deexcitation of ^{206}Pb (see previous section). Due to the low intensity of the 803.1 keV γ-ray, this method required more masses and longer irradiation time as compare to the previous described measurement.

A 146 mg wire of pure ^{209}Bi was enclosed in a 3 mm in diameter sealed quartz-capillary in order to avoid any mass loss of Po. The dimension of the wire was 1 mm in diameter and 10 mm in length what makes the γ self-shielding negligible. The capillary was placed in an Al container, as described in the previous section, with a (7.58 ± 0.01) mg foil of Al-0.1%Co alloy encapsulated in an identical quartz-capillary. The dimension of the alloy in the capillary was 1 mm in diameter and 6 mm in length. The irradiation was done for 7 days and followed by 184 days of cooling. Measurements were performed during 14 days to gather enough statistics in the γ-peak of interest.

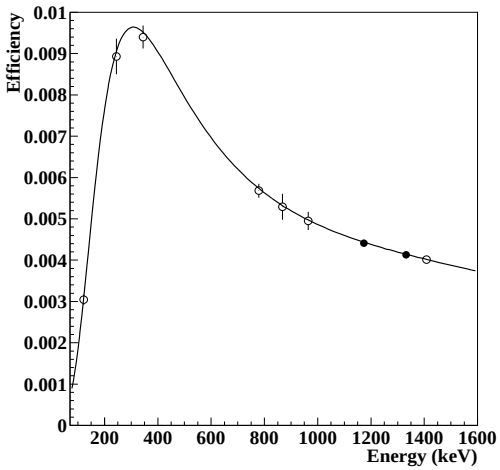

Fig. 6. Efficiency (intrinsic efficiency + solid angle) curve of the Ge-detector measured with ^{152}Eu (open circles) and ^{60}Co sources (full circles). Interpolation of the efficiency has been done by adjusting a logarithmic polynomial function on the data (line). A coaxial Ge-detector mounted in front of our detector was responsible for the decrease of the efficiency below 300 keV.

The 803.1 keV γ-ray has been collected with a Ge-detector which has an intrinsic efficiency of 10% for the 1173 keV γ-ray and an energy resolution of 2.5 keV. For this special low counting-rate measurement, the detector was completely shielded with lead bricks to reduce the background-counting rate to 0.03 counts/s at 800 keV. The total efficiency of the detector (intrinsic efficiency and solid angle) has been calibrated with ^{152}Eu and ^{60}Co standard point-like sources (Fig. 6) placed in front of the Ge-detector at approximately

3 cm from the Ge-crystal. The exact position of the sources was not precisely determined but strictly respected for both calibration sources, flux monitor (see section 3.3) and Bi-sample. As shown on Fig. 6 the total efficiency was sufficiently low to consider each hit involving a single γ-ray. This assumption was validated by looking at the peak-sum of the two γ-rays emitted by the ^{60}Co calibration source counting for less than 0.3% of the single rates.

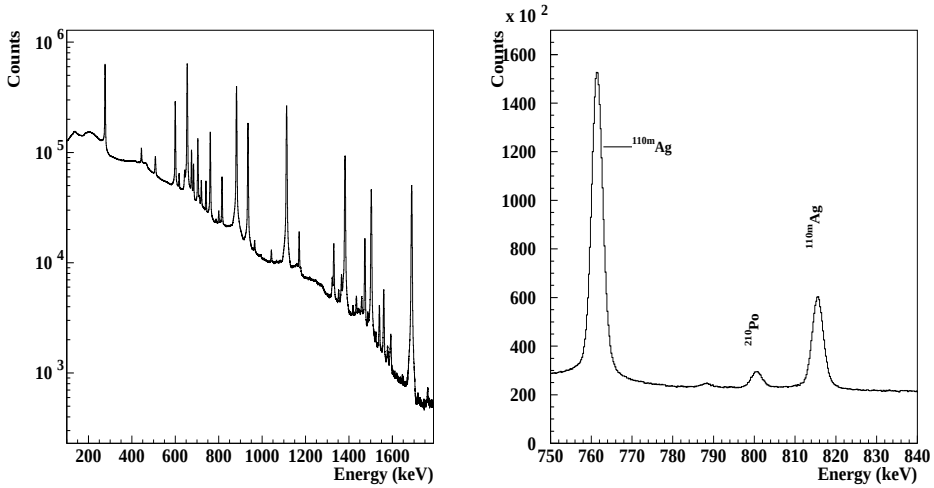

Fig. 7. a) Left: γ-energy spectrum collected with the Ge-detector after 7 days. b) Right: Zoom-in on the peak of interest.

The energy spectra, obtained after 7 days of measurement, is shown on Fig. 7a with a zoom-in on the 803.1 keV energy region (Fig. 7b). As shown on the figures, impurities contained in the sample are responsible for the majority of the counting rate and of the high compton background which amount to about 3/4 of the counts under the peak of interest. A sum of two asymmetric gaussian functions with a linear background was used to determine the number of counts in the peak. All the parameters were adjusted on neighboring peaks except the energy and the height of the peak. The result of the adjustment with this function on the ^{210}Po data gives an activity of (2140 ± 42) kBq.

3.3 Neutron flux measurements

The neutron flux was determined (Eq. 2) from the activities of the ^{59}Co monitors irradiated in exactly the same conditions as samples. In both experiments, the two 1173.24 and 1332.50 keV γ-rays accompanying the decay of the ^{60}Co nucleus were collected with high purity Ge detectors.

In the α-spectroscopy measurement, we have used the Ge detector from the Mini-Inca set-up (Marie et al.,2005) with an intrinsic photopeak efficiency of 9.8% and an energy resolution of 1.8 keV for the 1173 keV γ-ray. Measurements

have been done at different positions from the target to reduce statistical errors on the determination of the solid angle.

In the γ-spectroscopy measurement, we have used the same Ge detector than used for the measurement of the Bi-sample. The monitor was placed exactly at the same position as the Bi-sample (in closed contact to the crystal of the detector) so that the difference in the solid angles was negligible.

Activities of (62.7±1.2) kBq and (140.4±2.8) kBq were found for the monitors after 3 and 7 days of irradiation. When corrected for the masses of the monitors and assuming a maxwellian distribution corresponding to a temperature of 20 ^{o}C ($\overline{\sigma}_{Co}$ =(32.96 ± 0.06) b, Marie et al., 2005), we found values of (2.32 ± 0.06) 10^{13} n/cm^2/s and (2.34 ± 0.06) 10^{13} n/cm^2/s, respectively, for the fluxes. The main errors on the flux determination were due to the errors on the mass fraction of ^{59}Co in the Al foil (2%) and the measured activities (2%). We have to stress that the compatibility of these flux measurement results with previous measurements (Fioni et al., 2001) confirms a very good stability of the neutron flux at the T4 position.

4 Results and discussions

4.1 ^{210}Po ($^{210gs}Bi$) formation cross sections

The ^{210}Po formation cross section was obtained from the Eq. 3 by identifying it with the $^{209}Bi(n,\gamma)^{210gs}Bi$ cross section with a small error being less than 0.2%. Taking σ_{Co} =(37.18 ± 0.06) mb (Vonach et al., Zolotarev, 2002) at 0.0253 eV, we obtained values of σ_{gs} =(16.08 ± 1.8) mb and σ_{gs} =(18.4 ± 0.9) mb for the α and γ-spectroscopy methods respectively. The two results are compatible within the error bars. One possible explanation for the small difference could lie in a small release of ^{210}Po from the ^{209}Bi target in the case of the α-spectroscopy method, whereas in the case of the second measurement, the release was forbidden by the sealed quartz-capillary. The processes on how polonium can evaporate from a solid Bi target have been studied and described in Pankratov et al., (2003). In this paper, where a specific calculation was done for our work, it was shown that, in our experimental conditions of expected temperature (less than 250 ^{o}C), pressure (less than 1.8 bar) and gaz composition, not more than 1% of the created ^{210}Po could be lost even in the most penalising scenario. The results of these calculations, for three conditions of temperature during the irradiation, are presented in the Table 1.

We have to stress here that polonium evaporation is one of the main uncertainty in a LB target in operation. From our experiment we can not conclude

Parameters	Irradiation temperatures		
	150 ^{o}C (423 K)	200 ^{o}C (473 K)	250 ^{o}C (523 K)
$< G(\mathrm{T})>$ (Bq/s)	1.5 10^{-9}	1.0 10^{-6}	1.05 10^{-4}
ϵ(T) (%)	4.5 10^{-6}	2.9 10^{-3}	3.1 10^{-1}

Table 1
Average evaporation rate (<G(T)>) and relative loss (ϵ(T)) of polonium as a function of the target temperature during 3 days of irradiation and 84 days of cooling.

on the absence of evaporation of polonium but only say that the relative loss is smaller than error bars of the two experiments and confirm the calculations in a temperature range where a small quantity of polonium is expected to be loss. These calculations should be tested in more realistic experimental conditions with a temperature closed to the nominal temperature of a LB loop (i.e. 350 ^{o} C) and a longer irradiation time.

We have adopted a mean value of (17.9 ± 0.8) mb for the $^{209}Bi(n,\gamma)^{210gs}Bi$ cross section (i.e. ^{210}Po formation cross section). For this evaluation, we have increased the uncertainty on the cross section obtained from the first method, to take into account the uncertainty on the release of ^{210}Po.

Element	$T_{1/2}$	$\sigma_{work}(mb)$	$\sigma_{old}(mb)$	$\sigma_{eval}(mb)$
^{210}Po	138.376 (0.002) d	17.9 (0.8)		
^{210gs}Bi	5.013 (0.005) d	17.9 (0.8)	15.0 (3) Seren et al., (1947) 20.5 (1.5) Colmer et al., (1950) 24.2 (0.4) Takiue et al., (1978)	24.2 (0.4)

Table 2
Formation cross sections obtained in this work (σ_{work}) and compared with old measurements (σ_{old}) and evaluated value (σ_{eval}) from ENDF-BVI. Errors are indicated in brackets.

Our results are summarised in Table 2 and compared with evaluated values and old measurements. It appears that the value obtained in this work for the $^{210gs}Bi$ (i.e. ^{210}Po) formation cross section is compatible, with respect to the error bars, with very old activation measurements done by Seren et al., (1947) $(15 \pm 3$ mb) and Colmer et al., (1950) $(20.5 \pm 1.5$ mb). But, it is by 25% smaller than the most recent measurement done by Takiue et al (1978) $(24.2 \pm 0.4$ mb) and therefore by 25% smaller than the evaluated partial cross section based on this latter measurement. We do not have found any satisfying explanation about the discrepancy between their measurement, based on a direct collection of the β-decay of $^{210gs}Bi$, and our present work. Recently,

two direct measurements of the branching ratio between the ground and the metastable states by γ-spectroscopy (Letourneau et al., (2002) and Borella et al., (2004)) have confirmed the present value and shown also a subestimation of the ^{210m}Bi production branch by evaluations.

4.2 Po production in a Bi target

As a consequence of the difference between the evaluated and our recommended cross section, we could expect a reduction of at least 25% in the assessment of the ^{210}Po production in a LB spallation target when using the new value.

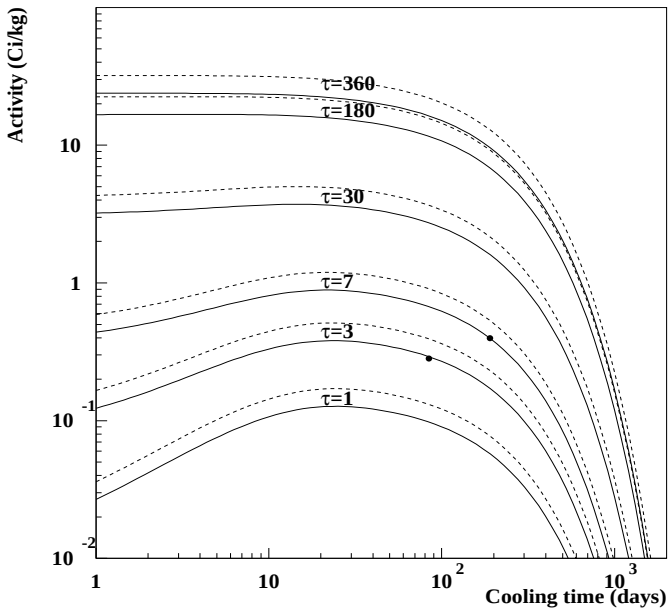

Fig. 8. Assessment of ^{210}Po activity (expressed in Ci for 1 kg of ^{209}Bi) for a Bi target irradiated in our experimental conditions of flux, as a function of cooling time and for different irradiation times (τ). For each irradiation time our recommended cross section (continuous line) is compared with the evaluated one (dashed line). Our experimental points are also printed out (symbols). Error bars are contained within the size of the symbols

In order to check this hypothesis and the impact of our new value on the ^{210}Po activity in a Bi(PbBi)-target, we have made an extrapolation from our experimental activities to the long-term irradiations. The calculated results, using Eq. 1, are presented in Fig. 8 as a function of cooling time, for different irradiation times (τ) and values of cross section (continuous lines are our recommended value while dashed lines are evaluated ones). Calculations have been made for a thermal neutron flux of 2.33 10^{13} n/cm^2/s (at 20 ^{o}C) and the

activity has been normalised to 1 kg of Bi. We think that the study presented in this section could be easily applied to a LB-spallation target surrounded by a moderator (with a non-negligible thermal component) in return for simply a scaling of the flux intensities.

It appears, on Fig. 8, that the impact of our new recommended cross section on the Po-activity assessment is even better than a reduction of 25%. After one year of irradiation, the activity deduced from the new value is almost the same than the activity estimated with the old value after 6 months of irradiation. This increasing in the gain factor, which appears after 30 days of irradiation, is due to the non-linearity in the relation between the time of irradiation and the quantity of ^{210}Po produced. The origin of the non-linearity lies in the compensation effect between the feeding and the decay of the ^{210}Po nuclei. On Fig. 8, this effect is visible after 30 days of irradiation when the evolution of the activity as a function of the cooling time becomes flat, showing a saturation in the production of ^{210}Po.

We have to stress that the importance of the new recommended partial cross section to estimate the radiotoxicity of a LB target depends drastically on the neutron energy spectra and on the importance of the thermal component. Thus, in order to get a precise evaluation of the production of ^{210}Po in a LB-target, a more precise simulation should be done with more realistic geometries for the target and for the moderator surrounding the target.

5 Conclusion

In this work, the cross section for the ^{210}Po production in the irradiation of a solid ^{209}Bi target in a pure thermal neutron flux has been measured by two distinct and direct experimental methods. The two methods give comparable results compatible with the older measurements, showing that experimental bias are small and in particular the evaporation of ^{210}Po from the target. The new value measured in our work is by 25% smaller than the used data-library values for the ^{210}Po production. As a consequence we can suspect that the evaluation of ^{210}Po production in a moderated Pb-Bi spallation target using these data-libraries will be over-estimated by at least 25% (we have shown that it could reach 50% for long-term irradiations). In order to complete this work and to check the validity of this hypothesis in a Pb-Bi spallation target, cross section measurements will be extended soon over the full energy range encountered in a spallation target at the Gelina facility (in Geel, Belgium).

Acknowledgements

These experiments would not have been possible without the co-operation and the essential help of the personnel of the ILL-Grenoble. We wish to acknowledge the ILL reactor division for the efficient technical support.

References

Borella, A., Schillebeeckx, P., Molnar, G., Belgya, T., Revay, Zs., Szentmiklosi, L., Berthoumieux, E., Gunsing, G., Letourneau, A., 2004. Proceeedings of International Conference on Nuclear Data for Science and Technology, 26 September - 1 October 2004, Santa Fe, United States.

Briesmeister, J., for Group X-6, 1993. LANL, preprint LA-12625-M.

Browne, E., 1992. Nucl. Data Sheets 65 209.

Colmer, F.C.W., 1950. Proceeding of the Physical Society A63 1175.

Deruelle, O., Cribier, M., Fadil, M., Faust, H., Fioni, G., Leconte, Ph., Marie, F., Martino, J., Ridikas, D., Veyssiere, C., 2000. Proceedings of the 8th Int. Seminar on Interaction of neutrons with matter, October, JINR Dubna, Russia.

Deruelle, O., 2002. Ph.D. thesis, University Paris XI (unpublished).

Fioni, G., Cribier, M., Marie, F., Aubert, M., Ayrault, S., Bolognese, T., Cavedon, J.-M., Chartier, F., Deruelle, O., Doneddu, F., Faust, H., Gaudry, A., Gunsing, F., Leconte, Ph., Lelievre, F., Martino, J., Oliver, R., Pluquet, A., Röttger, S., Spiro, M., Veyssiere, Ch., 2001. Nucl. Phys. A693 546.

Gai, E.V, Ignatyuk, A.V., Lunev, V.P., Shubin, Yu.N., 2000. Proceedings of the conference on Hadrons, Nuclei and Applications, 29 May - 3 June 2000, Bologna, Italy.

Harmatz, B., 1981. Nucl. Data Sheets 34 735.

Harris, S.P. et al., 1950. Phys. Rev. 80 342.

Igashira, M., Saito, K., Kawakami, J., Ohsaki, T., Sekimoto, H., 2001. Proceedings of the Korean Nuclear Society Spring Meeting, May 2001, Cheju, Korea.

Letourneau, A., Galin, J., Goldenbaum, F., Lott, B., Peghaire, A., Enke, M.,

Hilscher, D., Jahnke, U., Nünighoff, K., Filges, D., Neef, R.D., Paul, N., Schaal, H., Sterzenbach, G. and Tietze, A., 2000. Nucl. Inst. Meth. B 170 299.

Letourneau, A., Berthoumieux, E., Deruelle, O., Fadil, M., Fioni, G., Gunsing, F., Marie, F., Perrot, L., Ridikas, D., Boerner, H., Faust, H., Mutti, P., Simpson, G., Schillebeeckx, P., 2002. Proceedings of the 11th symposium on Capture γ-Ray Spectroscopy, 2-6 Sept. 2002, Prague, Czech Republic.

Marie, F., Letourneau, A., Fioni, G., Deruelle, O., Veyssiere, Ch., Faust, H., Mutti, P., Al Mahamid, I., Muhammad, B., 2005. Accepted for publication in Nucl. Instr Meth. A.

Pankratov, D., Ignatiev, S., Ridikas, D., Letourneau, A., 2003. Annals of Nuclear Energy 30 785.

Salvatores, M., Bauer, G.S. and Heusener, G., 1999. Report MPO-1-GB-6/0-GB, Paul Scherrer Institute, Zurich.

Seren, L., Friedlander, H.N., Turkel, S.H., 1947. Phys. Rev. 72 888.

Takiue, M. and Ishikawa, H., 1978. Nucl. Instr. Meth. 148 157.

Vonach et al., Zolotarev, K.I., 2002, IRDF2002, www.nndc.bnl.gov/nndcscr/libraries/irdf/.